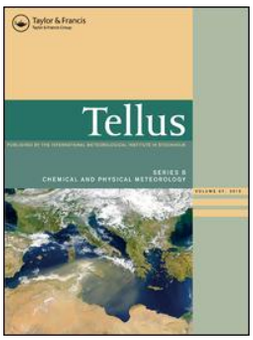

Tellus B: Chemical and Physical Meteorology

ISSN: (Print) 1600-0889 (Online) Journal homepage: http://www.tandfonline.com/loi/zelb20

Hygroscopic properties of aerosol particles in the north-eastern Atlantic during ACE-2

Erik Swietlicki, Jingchuan Zhou, David S. Covert, Kaarle Hämeri, Bernhard Busch, Minna Väkeva, Ulrike Dusek, Olle H. Berg, Alfred Wiedensohler, Pasi Aalto, Jyrki Mäkelä, Bengt G. Martinsson, Giorgos Papaspiropoulos, Besim Mentes, Göran Frank & Frank Stratmann

To cite this article: Erik Swietlicki, Jingchuan Zhou, David S. Covert, Kaarle Hämeri, Bernhard Busch, Minna Väkeva, Ulrike Dusek, Olle H. Berg, Alfred Wiedensohler, Pasi Aalto, Jyrki Mäkelä, Bengt G. Martinsson, Giorgos Papaspiropoulos, Besim Mentes, Göran Frank & Frank Stratmann (2000) Hygroscopic properties of aerosol particles in the north-eastern Atlantic during ACE-2, Tellus B: Chemical and Physical Meteorology, 52:2, 201-227, DOI: 10.3402/tellusb.v52i2.16093

To link to this article: https://doi.org/10.3402/tellusb.v52i2.16093

Published online: 15 Dec 2016.

Tellus (2000), 52B, 201–227
Printed in UK. All rights reserved

TELLUS
ISSN 0280–6509

Hygroscopic properties of aerosol particles in the north-eastern Atlantic during ACE-2

By ERIK SWIETLICKI[1]*, JINGCHUAN ZHOU[1], DAVID S. COVERT[3], KAARLE HÄMERI[2], BERNHARD BUSCH[4], MINNA VÄKEVA[2], ULRIKE DUSEK[3], OLLE H. BERG[1], ALFRED WIEDENSOHLER[4], PASI AALTO[2], JYRKI MÄKELÄ[2], BENGT G. MARTINSSON[1], GIORGOS PAPASPIROPOULOS[1], BESIM MENTES[1], GÖRAN FRANK[1] and FRANK STRATMANN[4], [1]*Division of Nuclear Physics, Lund University, PO Box 118, S-221 00 Lund, Sweden;* [2]*Department of Physics, PO Box 9, University of Helsinki, FIN-00014 Helsinki, Finland;* [3]*University of Washington, Department of Atmospheric Sciences, Box 354235, Seattle, WA 98195-4235, USA;* [4]*Institute for Tropospheric Research, Permoser Str. 15, D-04303, Leipzig, Germany*

(Manuscript received 5 February 1999; in final form 17 September 1999)

ABSTRACT

Measurements of the hygroscopic properties of sub-micrometer atmospheric aerosol particles were performed with hygroscopic tandem differential mobility analysers (H-TDMA) at 5 sites in the subtropical north-eastern Atlantic during the second Aerosol Characterization Experiment (ACE-2) from 16 June to 25 July 1997. Four of the sites were in the marine boundary layer and one was, at least occasionally, in the lower free troposphere. The hygroscopic diameter growth factors of individual aerosol particles in the dry particle diameter range 10–440 nm were generally measured for changes in relative humidity (RH) from $<10\%$ to 90%. In the marine boundary layer, growth factors at 90% RH were dependent on location, air mass type and particle size. The data was dominated by a unimodal growth distribution of more-hygroscopic particles, although a bimodal growth distribution including less-hygroscopic particles was observed at times, most often in the more polluted air masses. In clean marine air masses the more-hygroscopic growth factors ranged from about 1.6 to 1.8 with a consistent increase in growth factor with increasing particle size. There was also a tendency toward higher growth factors as sodium to sulphate molar ratio increased with increasing sea-salt contribution at higher wind speeds. During outbreaks of European pollution in the ACE-2 region, the growth factors of the largest particles were reduced, but only slightly. Growth factors at all sizes in both clean and polluted air masses were markedly lower at the Sagres, Portugal site due to more proximate continental influences. The frequency of occurrence of less-hygroscopic particles with a growth factor of ca. 1.15 was greatest during polluted conditions at Sagres. The free tropospheric 50 nm particles were predominately less-hygroscopic, with an intermediate growth factor of 1.4, but more-hygroscopic particles with growth factors of about 1.6 were also frequent. While these particles probably originate from within the marine boundary layer, the less-hygroscopic particles are probably more characteristic of lower free tropospheric air masses. For those occasions when measurements were made at 90% and an intermediate 60% or 70% RH, the growth factor $G(\mathrm{RH})$ of the more-hygroscopic particles could be modelled empirically by a power law expression. For the ubiquitous more-hygroscopic particles, the expressions $G(\mathrm{RH}) = (1 - \mathrm{RH}/100)^{-0.210}$ for 50 nm Aitken mode particles and $G(\mathrm{RH}) = (1 - \mathrm{RH}/100)^{-0.233}$ for 166 nm accumulation mode particles are recommended for clean marine air masses in the north-eastern Atlantic within the range $0 < \mathrm{RH} < 95\%$, and for wind speeds for which the local sea-salt production is small ($<$ ca. 8 m s^{-1}).

* Corresponding author.
e-mail: Erik.Swietlicki@nuclear.lu.se

1. Introduction

1.1. The rôle of measurements of hygroscopic properties of aerosol particles within ACE-2

The interaction of tropospheric aerosol particles with the ubiquitous water vapour largely determines the effects of the aerosol on the environment and its life-time and removal mechanisms. The hygroscopic properties of the aerosol particles control their water content and thereby the actual size of the individual aerosol particles at a given ambient relative humidity (RH). The water content influences the aqueous phase chemistry as well as the optical properties of the aerosol. At water vapour supersaturations typical of stratus and stratocumulus clouds, the hygroscopic properties are vital in determining which particles will act as cloud condensation nuclei (CCN) or remain as an interstitial aerosol.

The Intergovernmental Panel on Climate Change (IPCC) clearly recognises the importance of atmospheric aerosols in the global radiative balance, and conclude that aerosols currently constitute the largest source of uncertainty in predictions of the future global climate (IPCC, 1995). The atmospheric aerosol can influence the radiative balance directly through the upward scattering and absorption of incoming short-wave solar radiation (which depend on ambient size and optical properties) or indirectly through the rôle of aerosol particles as CCN. The nature and abundance of the available CCN affect the cloud microphysical structure and life-time of the clouds and thereby the global cloud albedo.

The second Aerosol Characterization Experiment (ACE-2) was conducted in the anthropogenically influenced marine atmosphere of the north-eastern Atlantic between 16 June–25 July 1997 (Raes et al., 2000; Verver et al., 2000). The goal of ACE-2 is to determine and understand the properties and controlling factors of the aerosol in the anthropogenically modified atmosphere of the north-eastern Atlantic and assess their relevance for radiative forcing.

Clearly, the hygroscopic properties of the aerosol particles are of vital importance for both the direct and indirect forcing of global climate by aerosols. Altogether, the life cycle of the atmospheric aerosol and its constituents cannot be fully understood and modelled unless the hygroscopic properties are adequately characterised and parameterised. Reversing the argument, the observed hygroscopic properties of aerosol particles can be used as a sensitive indicator for the ability of aerosol dynamics models to account for the aerosol evolution.

In an effort to contribute to the fulfilment of the ACE-2 objectives, continuous in-situ measurements of the hygroscopic properties of individual sub-micrometer particles using Hygroscopic Tandem Differential Mobility Analysers (H-TDMA, see description below) were performed at five different locations in the north-eastern Atlantic region during the ACE-2 experiment.

The four major aerosol types of the north-eastern Atlantic region are: (i) sea-salt particles; (ii) dimethyl sulphide (DMS)-derived particle mass; (iii) Saharan mineral dust, and (iv) outbreaks of anthropogenic pollution from Europe and North America 1997 (Raes et al., 2000; Verver et al., 2000). These aerosol types can exist as either an internal mixture, where all particles of a specific size have identical chemical composition, or an external mixture, which in its extreme means that all particles differ from one another chemically. Measurements of the hygroscopic properties of individual aerosol particles with H-TDMA instruments are efficient in revealing the aerosol mixing state as a function of particle size and time.

1.2. Previous observations of the hygroscopic properties of aerosol particles in various environments

Previous studies of the hygroscopic properties of atmospheric aerosol particles using H-TDMA instruments (McMurry and Stolzenburg, 1989; Zhang et al., 1993; Svenningsson et al., 1997; Swietlicki et al., 1997; Berg et al., 1998; Swietlicki et al., 1998) have shown that sub-micrometer atmospheric aerosol particles exhibit a modal hygroscopic structure, in the sense that a continuum of hygroscopic growth factors (relative particle diameter increase from dry to humidified state) is not observed. Instead, one, two or even more modes of hygroscopic growth have been observed to appear simultaneously. The atmospheric aerosol is therefore in many cases externally mixed regarding its hygroscopic properties

and hence also chemically. The observed groups of particles are normally denoted the less-hygroscopic mode, the more-hygroscopic mode and a separate mode caused by externally mixed sea-salt aerosol. Nearly hydrophobic particles have also been observed at numerous occasions when the sampling sites were influenced by fresh combustion aerosol.

In continental polluted aerosols, the particles generally separate into a less- and a more-hygroscopic group. The more-hygroscopic particles show diameter growth factors (dry to RH = 90%) in the range 1.3–1.8. This growth is in general less than the growth expected for pure salts of the major ions making up the aerosol particles, indicating that even the particles in this more-hygroscopic group consist of both water-soluble and insoluble or slightly soluble material with the less soluble fraction as large as half of the mass.

Prior to the ACE-2 experiment, ship-based measurements have been carried out during cruises over the Pacific and Southern Oceans in connection with the ACE-1 experiment (Berg et al., 1998), and on the Swedish icebreaker Oden during the Arctic Ocean Expedition 1996 (Swietlicki et al., 1998). In marine air masses, externally mixed sea salt particles appear at wind speeds $>$ ca. 10 m s^{-1}. The measured growth factors (dry to RH = 90%) of between 2.0–2.3 are similar to those of pure NaCl (2.4). These freshly produced sea-salt particles could be found as small as 50 nm in diameter. In these air masses, the more-hygroscopic mode is largely sulphate compounds derived from the oxidation of dimethyl sulphide (DMS), with growth factors (dry to RH = 90%) similar to those expected from mixtures of ammonium and sulphate ions with various degrees of acid neutralisation, i.e., 1.6–1.8. Atmospheric processing of freshly produced sea salt particles result in mixtures consisting primarily of sodium, chloride, sulphate and ammonium ions and organic compounds from gas phase deposition, causing a gradual decrease in growth factors (at RH = 90%) from around 2.3 to 1.6–1.8.

2. Description of H-TDMA principle and operation

2.1. *H-TDMA measurements of hygroscopic properties*

The measurement of the hygroscopic properties of sub-micrometer atmospheric aerosol particles was performed with 6 Hygroscopic Tandem Differential Mobility Analysers (H-TDMA) at 5 sites in the subtropical north-eastern Atlantic during the ACE-2 experiment. Although the instruments of the different participating groups were not of identical design and manufacture, they all operated according to the same general principle.

An H-TDMA as used in the ACE-2 experiment determines, in-situ, the hygroscopic growth of individual aerosol particles in terms of their change in diameter when they are taken from a dry, low relative humidity (generally $<$ 10% RH) to a hydrated state at a controlled higher RH, nominally 85 to 90%. The H-TDMA consists of three main parts: (1) a Differential Mobility Analyser (DMA1) which selects a narrow, quasi-monodisperse size range out of the full atmospheric aerosol size distribution at low RH, (2) humidifiers which condition the air to a specified, controlled higher RH and (3) a second DMA (DMA2) which measures the distribution of the change in diameter caused by the imposed humidification. During normal operation, the humidity in DMA2 is kept constant (e.g., at RH = 90%), but it can also be varied so that atmospheric aerosol particles showing RH hysteresis behaviour (deliquescence and efflorescence) can be studied.

2.2. *Hygroscopic growth distribution and growth factor*

The individual particles in a sample population of atmospheric aerosol at a given dry diameter will generally have a distribution of chemical composition, and thus will have a distribution also of hygroscopic properties that may range from hydrophobic (water insoluble and non-wettable) to slightly soluble to highly hygroscopic or totally water soluble. The H-TDMA determines this distribution of hygroscopic properties by measuring growth as described above. As described in Section 1, it has been observed that the data exhibit one or more discrete, relatively narrow growth modes rather than a broad distribution of growth. Thus, it is expedient and accurate to describe the results in terms of modal values of the growth distribution, e.g., diameter growth factor. The hygroscopic growth factor is a diameter ratio defined as the particle diameter of a growth mode at the elevated, DMA2 RH (e.g., 90%)

divided by the particle diameter at the lower, DMA1 RH (e.g. $<10\%$). For completely hydrophobic particles this growth factor is obviously unity (1).

The modes are determined by fitting the distribution after an inversion procedure that accounts for the instrumental broadening of the modes caused by the finite width of the transfer functions of the DMAs. For simplicity, it is often assumed that the growth factors within each group of particles are normally distributed. The data inversion can then be performed with the TDMAFIT fitting program (Stolzenburg and McMurry, 1988) or other varieties (Stratmann et al., 1997).

The primary parameters measured by the H-TDMA and estimated by the data inversion routine for each group of particles showing similar hygroscopic growth are: (i) Arithmetic mean diameter growth factor; (ii) Diameter growth dispersion factor, and; (iii) Number fraction of particles in each hygroscopic particle group.

2.3. Operational parameters

Table 1 shows a summary of the operational characteristics of the various H-TDMA instruments during ACE-2. The two UHEL instruments were mainly focused on studying the hygroscopic behaviour of ultrafine particles at a dry size of 10 nm, and the Izaña instrument operated at a dry particle size of 50 nm only for limited time periods. The IfT, ULU and UWA instruments covered the Aitken (35, 50, 73 nm) and accumulation (100, 109, 150, 166, 250, 264, 440 nm) mode size ranges.

All but the UHEL H-TDMA instrument used aerosol humidifiers (Table 1). The particles exiting DMA1 had therefore spent 1–2 s at elevated humidity before entering DMA2. Water vapour equilibration times are very short, normally milliseconds or shorter for sub-micrometer particles, even when the accomodation coefficient is reduced substantially by surfactants (Kerminen, 1997). It is therefore likely to assume that water-inhibiting substances did not affect the growth of particles by humidification in a way that affected the H-TDMA measurements.

The standard measurement routine of the ULU instrument was that the growth factors were determined at RH = 90%, while every 6th h, the growth factors at 50 and 166 nm were also measured at RH = 70% for the duration of one full hour. The UWA instrument also measured at a low RH (60%) once a day, both for increasing and decreasing RH. This enabled parameterisations of hygroscopic growth factors versus RH to be calculated.

One DMA2 scan at a given particle dry size took about 5–10 min to complete. For the sites where several dry diameters were studied, a complete series of scans lasted about 50 min.

2.4. Description of the sampling sites

Punta del Hidalgo, Tenerife (ES), 16°19′W, 28°34′N, 63 m asl. Measurements were performed at the lighthouse of Punta del Hidalgo, located directly on the shore-line on the NE tip of Tenerife. The common aerosol inlet was placed at the top of the lighthouse 63 m above sea level. The inlet was designed to prevent rain from entering the sampling line, but had no well-defined upper cut-off diameter. From the inlet, the air was drawn through a 55 m long vertical tube to ground level. The flow rate in the tube was $200\,l\,min^{-1}$ and sub-turbulent. It took about 5 min for the sampled air to travel to the bottom of the lighthouse. The sampling tube was at room temperature around 30°C. The ULU H-TDMA was placed in a room at ground level together with several other instruments.

A wind sector control system was operating to ensure that the data could be screened for local pollution sources. The clean-sector criteria were: (1) The wind direction was confined within a sector between $<80°$ and $>280°$, i.e., towards the open sea; (2) the wind speed was $>1\,m\,s^{-1}$, and; (3) the instantaneous particle concentration increased by less than $300\,cm^{-3}$ over the 30 min running average value. Satisfactory samples were typically only obtained during north-easterly trade wind conditions, i.e., wind directions 0°–80°.

Paiba, Tenerife (ES), 16°12′W, 28°32′N, 500 m asl. The data from this station will not be presented here. See Bower et al. (2000) for a description of the site and results from the ULU and UHEL H-TDMA instruments and their rôle in the ACE-2 hill cap cloud experiment.

Izaña, Tenerife (ES), 16°30′W, 28°18′N, 2367 m asl. The Izaña baseline observatory is operated by the Spanish Meteorological Institute, and is part of the WMO Global Atmosphere Watch network.

Table 1. *Summary of the various H-TDMA instruments and their operational characteristics during ACE-2*

Group	Platform	DMA type, length DMA1/DMA2 (m) (flow ratio in l min^{-1})	CPC1/CPC2 type (CPC flow in l min^{-1})	Dry sizes (nm)	Aerosol drier before DMA1	Aerosol humidifier before DMA2	RH (%)
IfT	R/V Vodyanitsky	Hauke, 0.60(1.75/17)/ 0.60(1/17)	TSI 3010(1.0)/ TSI 3010(1.0)	50, 100, 150, 250	No	Yes	75–80
UHEL	Paiba, Tenerife (ES) 16°12′W, 28°32′N 500 m asl	Vienna, 0.11(1/10)/ 0.11(1/10)	–/TSI 3010(1.0)	10	No	No	ca. 95
UHEL	Izaña, Tenerife (ES) 16°30′W, 28°18′N 2367 m asl	Vienna, 0.11(1/10)/ 0.11(1/10)	–/TSI 3010(1.0)	10, 50[1]	No	No	ca. 95
ULU	Punta del Hidalgo, Tenerife (ES) 16°19′W, 28°34′N 63 m asl	Vienna, 0.28(1.8/12.6)/ 0.50(1/7)	TSI 3760(0.8)/ TSI 3760A(1.0)	35, 50, 73, 109, 166, 264, 440	Yes	Yes	90, 70[2]
ULU	Paiba, Tenerife (ES) 16°12′W, 28°32′N 500 m asl	Vienna, 0.28(1.8/12.6)/ 0.50(1/7)	TSI 3760(0.8)/ TSI 3760A(1.0)	35, 50, 73, 109, 166, 264, 440	Yes	Yes	90, 70[2]
UWA	Sagres (P) 8°57′W, 36°59′N 50 m asl	TSI, 0.44(1.3/7)/ 0.44(1/5)	TSI 3760(0.3)/ TSI 3010(1.0)	35, 50, 100, 150, 250	Yes	Yes	90, 60[3]

IfT: Institute for Tropospheric Research, Leipzig Germany; UHEL: Dept. of Physics, University of Helsinki, Finland; ULU: Division of Nuclear Physics, Lund University, Sweden; UWA: Dept. of Atmospheric Sciences, University of Washington, Seattle, USA.
[1] 50 nm: 18–19 June, 18–25 July, 1997.
[2] Every 6th h, 1 h scanning at 50 and 166 nm.
[3] Once a day, both for increasing and decreasing RH.

It is also a site of the AEROCE programme. The station is on a mountain platform, 2367 m above sea-level, and is the only free tropospheric station in the North Atlantic region. During night-time, free tropospheric air subsides over Tenerife, whereas during daytime, up-slope winds develop and Izaña is exposed to marine boundary layer (MBL) air perturbed by local anthropogenic and biogenic emissions.

The UHEL H-TDMA operated on a separate aerosol inlet. Ambient air was sampled at a flow rate of 2 l min^{-1} through a 4 mm ID stainless steel tube from a height of 5 m above ground on the northern side of the station. The total length of the sampling line was about 3 m, of which 2.5 m was at room temperature. The particle counter (TSI model CPC 3010) after DMA2 operated with a saturator-condenser temperature difference of 25°C, resulting in a 50% particle detection efficiency size of 8 nm.

Sagres-50, (P), 8°57′W, 36°59′N, 50 m asl. Measurements were performed at the Portuguese Radionaval Base about 1 km north-west of the town of Sagres on the south-western tip of Portugal. The site was located 1 km from the western coast and 100 m from the southern coast, at an altitude of 50 m.

The nearby surroundings to the north-east through south-west are relatively unaffected by human activities. With northerly winds, however, the air masses were clearly affected by power plants and other anthropogenic activities at a distance of 50 to 200 km or further north along the western coast of Portugal. The predominant wind direction was from NNW.

The UWA H-TDMA was located in a container in which several other aerosol measurements were also made. The H-TDMA sampled from a common aerosol flow of 16.7 l min^{-1} through a low-flow Anderson PM10 inlet mounted 20 m above ground to avoid near-ground dust contamination. Inside the container, the sample was divided into several 4 mm ID lines. The line to the H-TDMA was about 3 m in length with a flow of 1 liter min^{-1}.

The ship R/V Vodyanitsky. The shipborne H-TDMA operated by IfT was located in a container on the port side of the deck on R/V Vodyanitsky (Institute of Biology of Southern Seas, Sebastopol, Ukrania). The ship functioned as a mobile sea surface measurement platform during ACE-2, and active sampling was performed during the period 20 June–23 July 1997 in the area between 29°–41°N and 8°–15°W.

A common inlet was used to sample aerosol particles at 10 m above sea level through a heated mast. The mast extended 6 m above the aerosol measurement container and was capped with a cone-shaped inlet nozzle that was rotated to point into the relative wind. At an ambient wind speed of 10 m s^{-1} air was sampled nearly isokinetically by this 5 cm diameter inlet nozzle at flow of 1 m^3 min^{-1} and then through the 20 cm inner diameter mast. The lower 1.5 m of the mast were heated to dry the aerosol to a relative humidity of 55%. 15 1.9-cm diameter conductive tubes extending from this heated zone were used to isokinetically withdraw flows from the larger air stream to the various aerosol instruments at flows of 30 l min^{-1}. One of these tubes was used to supply ambient air to the IfT H-TDMA along with other aerosol instrumentation. Periods of contamination from the ship were excluded from the data on the basis of relative wind and high particle counts.

3. Quality assurance procedures

To ensure that the H-TDMA data from the instruments at the different sites would be comparable, quality assurance procedures were determined in advance of the experiment and consistent data analysis procedures were followed after the experiment. Accurate measurement, control and monitoring of temperature, humidity and flow in the DMAs are needed for the determination of hygroscopic growth distributions. Because the combined effect of errors and uncertainty in all these parameters can be large and difficult to quantify, calibration with an aerosol of known chemical composition and growth factor at a given RH was needed as well.

All flows were checked daily with electronic bubble flow meters. For the ULU and UWA instruments, the aerosol sample flows in DMA1 and DMA2 were monitored by measuring the pressure drop across a flow restriction. DMA sheath and excess flows were either controlled by mass flow controllers or monitored by mass flow meters at least once during each growth measurement. The drift in the DMA sheath and excess flows was less than 2% and the drift in the DMA aerosol flows was less than 10%. The CPC (Condensation Particle Counter) flows were stable within 1%. The capacitive humidity sensors used for humidity control and RH measurements at multiple points in the systems were calibrated against a dew point hygrometer or psychrometer. The absolute error in the dew point hygrometer or psychrometer estimate of DMA2 RH is $\pm 1\%$ at RH = 90%. Humidities and temperatures at one or more locations representative of the condition in the mobility column of DMA2 were monitored for each measurement. DMA1 RH was $<15\%$ for the instruments where no aerosol drier was used, and $<10\%$ for the others.

The error in measured growth factor by the H-TDMA is estimated to be $\pm 3\%$ or ± 0.05 relative units for a growth factor of 1.8. This is a result of humidity fluctuations and humidity gradients in DMA2 and errors in modal values from

counting and curve fitting uncertainty. The smallest detectable number fraction of an externally mixed hygroscopic particle group is about 5%, for the case when the growth factor peaks are well separated. The function of the equipment was regularly checked for growth at the nominal RH with standard aerosol of pure ammonium sulphate or sodium chloride. The growth factor of the test aerosol agreed with modelled growth (Tang and Munkelwitz, 1994; Tang, 1997) within the error estimated above.

All particle counters were calibrated for counting efficiency as a function of size at the flows and temperatures of the respective H-TDMA systems in advance of the field campaign. The transfer functions of the DMAs were also determined experimentally prior to the experiment. These calibrations were performed either at the Institute for Tropospheric Research in Leipzig, Germany, or at each individual laboratory according to a common procedure.

The various H-TDMA instruments operated at different DMA2 RHs (Table 1), and also monitored humidities and temperatures differently. This meant that identical quality assurance criteria could not be used for all instruments. Table 2 gives an example of the criteria applied to the ULU H-TDMA data. Similar criteria were used to safeguard the data quality of the other H-TDMAs and comparability between instruments.

Incidents of local pollution were removed from the data according to the procedures given in the description of the various sampling sites (Subsection 2.4) or in the discussion of the results of the free tropospheric measurements (Subsection 5.4).

4. Growth factor correction

During operation of the various H-TDMA instruments, all possible efforts were made to ensure that the RH of DMA2 was stable and close to a nominal value. Post-experiment evaluation of instrument performances showed that for most of the time, the actual RH of measurement deviated somewhat from the nominal values, and furthermore, different nominal values were used for the various H-TDMA instruments. In order for an intercomparison to be made between the various H-TDMA measurements, the measured growth factors needed to be corrected from the actual DMA2 RH to some common RH value. Since the bulk of the data was acquired at an RH close to 90%, the measured growth factors were corrected to this common RH value.

Multiple filter and impactor measurements performed during ACE-2 show that $(NH_4)_x(SO_4^=)_y$ was a major sub-micrometer aerosol component for all sites (Putaud et al., 2000; Quinn et al., 2000; Neusüß et al., 2000). The correction of hygroscopic growth factors was made assuming that the soluble particle fraction consisted of ammonium bisulphate. In order to evaluate the sensitivity of the growth factor corrections to particle composition, corrections were also made assuming an ammonium sulphate soluble particle fraction. Although the diameter growth factors for a 150 nm particle

Table 2. *Quality assurance criteria used for acceptance of the ULU H-TDMA data*

Parameter	Criterion	Goal
DMA2 RH average during scan	87–94% RH	limit range for comparability and to allow correction to RH = 90%
DMA2 RH variability during scan	± 1% RH	minimize RH fluctuation during particle classification
sheath — excess flow temperature difference	± 0.3°C	minimize RH gradients in DMA2
CPC1 concentration	$< 50\ cm^{-3}$	eliminate periods of contamination
relative standard deviation in CPC1 concentration	< 0.4	particle concentration stable during scan
standard deviation of sheath flow RH	< 1% RH	DMA2 humidity control working properly
stability of DMA flows during scan	± 1% sheath	accurate size classification
	± 3% aerosol	accurate concentration measurement

All the criteria given in the table had to be fulfilled in order for a scan to be accepted. Similar criteria were used for the other H-TDMA instruments.

taken from a dehydrated state to RH = 90% is about 6% higher for pure ammonium bisulphate compared with that of ammonium sulphate, the resulting corrected diameter growth factors were almost identical for the two salts (within 1%). The reason for this is that the important quantity for the growth factor correction is the relative change of particle diameter to variations in RH around RH = 90% (i.e., dD_p/dRH), which are quite similar for the two salts, and not the exact value of the growth factor at the nominal RH.

The first step in the correction was to calculate the soluble particle volume fraction, assuming again that each particle consisted of ammonium bisulphate and a hygroscopically inactive core. The equations used for the calculations are presented in Swietlicki et al. (1999) for ammonium sulphate. The thermodynamic data needed for ammonium bisulphate are (i) water activity as a function of molality, and (ii) density as a function of molality (or weight fraction of solute). Empirical parameterisations of both these quantities, based on experiments performed with an electrodynamic balance, can be found in Tang and Munkelwitz (1994).

Once the soluble volume fraction is estimated (from the dry particle diameter, the observed diameter growth factor and the actual DMA2 RH during measurement), the diameter growth factor at the nominal RH can be calculated for a particle having the same dry diameter as the original particle, and with the estimated soluble volume fraction of ammonium bisulphate. This calculation of the diameter growth factor at the nominal RH is iterative in order to take into account the Kelvin effect, i.e., the lowering of the water activity of the aqueous solution over the curved particle surface.

The errors introduced by this correction are estimated to be $<1\%$, and are likely to be largest for the data taken at the ship and at Izaña, since these measurements were carried out at RHs which deviated more than a few % from 90%.

5. Results

Rather than presenting the H-TDMA data simply on a station-by-station basis, the collected data will most likely be of greatest value to the scientific community when classified and presented according to air mass type. By doing so, data can be compiled that is characteristic, not only for the region and season in question, but also for the various air mass types. Furthermore, it is valuable to extract any possible information relating to the evolution of the atmospheric aerosol particles. In the case of the hygroscopic properties, the available data allow averages for aerosol particles in different stages of their evolution to be calculated:

- freshly produced aerosol (local pollution);
- aged polluted continental aerosol (European outflow passing Sagres);
- polluted continental aerosol aged over ocean (European outflow reaching ship and/or Tenerife).

Since the rather low wind speeds resulted in low concentrations of newly formed and externally mixed sea-salt particles within the H-TDMA size ranges, the ageing of such sea-salt particles could not be studied. Instead, typical aged clean marine background air masses were characterised.

5.1. *Clean marine background air masses*

The time periods representing clean marine background air masses were chosen according to 4 criteria:

1. air mass back trajectories confined to the Atlantic or Arctic Oceans for the entire length of the trajectory (5 days);
2. no local pollution;
3. no or limited (Sagres) signs of aged pollution;
4. H-TDMA quality assurance criteria fulfilled.

This selection procedure resulted in the overall time periods for the clean marine air masses at the various MBL sites shown in Table 3.

Growth factors for the more-hygroscopic particles calculated in these clean marine air masses are presented in Fig. 1. Also shown in this Figure are the corresponding averages for the more-hygroscopic particles as measured on the ship R/V Discoverer during the ACE-1 campaign (Berg et al., 1998). The ACE-1 data was corrected to RH = 90% (Pacific Ocean data originally at RH = 89%). Only periods without pollution were included in the ACE-1 Pacific Ocean data. For the Southern Ocean, the average for the entire ACE-1 intensive was used. The clean marine air mass data for all particle groups are summarised in Tables 5–7.

Table 3. *Time periods selected as clean marine air masses (1 January 1997 at noon is DOY = 1.5) at the various MBL sites*

Clean marine air masses					
Hidalgo		Sagres		ship	
day of Year	start date	day of year	start date	day of year	start date
167	16 June	172.83–173.50	21 June	173.5–174.7	22 June
169	18 June	177.50–178.40	26 June	177.5–181.5	26 June
171	20 June	179.10–179.80	28 June	183.5	2 July
173–179	22 June	180.00–181.20	29 June	186.2	5 July
183–186	2 July	184.00–185.00	3 July	192.5–193.5	11 July
193–197	12 July			201.2–202	20 July
204–205	23 July				

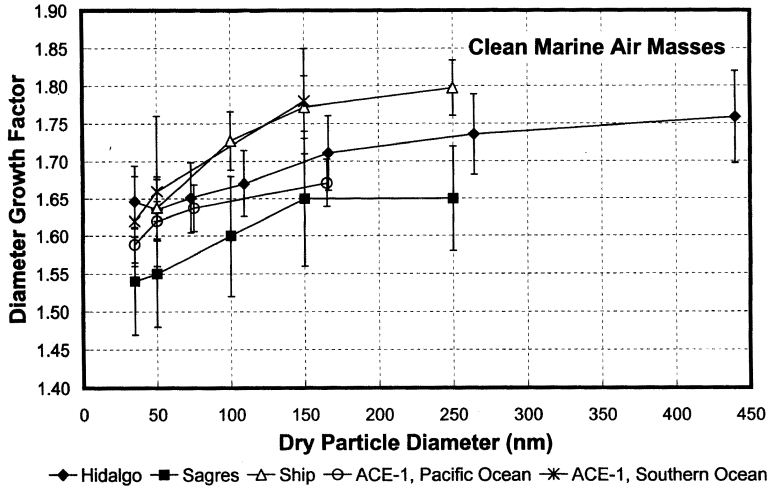

Fig. 1. Hygroscopic diameter growth factor averages ± one standard deviation (at RH = 90%) for the clean marine periods at Hidalgo (Tenerife), Sagres (Portugal) and the ship. For comparison, the corresponding data taken over the Pacific and Southern Oceans during the ACE-1 experiment are also shown.

The growth factors increase slightly with increasing particle diameter. Assuming identical chemical composition over the entire size range, the Kelvin effect alone is sufficient to explain this increase for the Punta del Hidalgo and Sagres sites, but not for the ship.

5.2. *Continental influence — European outbreaks*

One of the main objectives of ACE-2 is to study the evolution of the polluted European plume as it advected over the Atlantic Ocean. During three Lagrangian experiments, the air mass was tracked by constant level balloons over a distance of more than 1000 km, guiding the Meteorological Research Flight's C-130 aircraft while performing a comprehensive suite of aerosol and gas measurements (Johnson et al., 2000). However, these airborne measurements did not include the hygroscopic properties of the aerosol particles. The MBL H-TDMA measurements at the several sites can partly compensate for this shortcoming.

During ACE-2, there were unfortunately no occasions for which one and the same air mass passed over all three MBL sites (Sagres, ship, Hidalgo). Instead, periods when each of the sites had been affected by a well-mixed European plume outbreak had to be defined. Even though this

meant that slightly different air masses were actually studied at the various sites, the combined average results could nevertheless be interpreted as having been derived from a Lagrangian-type experiment. The time periods representing European plume outbreaks were chosen according to three criteria:

1. air mass back trajectories originating from over Spain and/or France;
2. well-mixed air masses with no or insignificant signs of local pollution;
3. H-TDMA quality assurance criteria fulfilled.

This selection procedure resulted in the overall time periods for the European plume outbreaks at the various MBL sites shown in Table 4. Growth factors for the more-hygroscopic particles calculated during these time periods are presented in Fig. 2.

The first two Sagres periods are a subset of the 3rd European pollution outbreak into the ACE-2 region during the experiment (DOY 185–191 in Sagres), and the last Sagres period is a subset of the 5th outbreak (DOY 195–205) as defined by Raes et al. (2000). The criterion of insignificant local or nearby pollution disqualified the other ACE-2 pollution outbreak time periods defined by Raes et al. (2000), since the purpose here was to study a well-mixed continental plume which had aged over half a day or more at all three sites. The 3rd ACE-2 pollution outbreak was the first pollution event throughout the ACE-2 domain and reached Tenerife 36–40 h later. The 5th ACE-2 pollution outbreak (DOY: 195–205) led to two separate pollution events at Punta del Hidalgo (DOY: 198–203 and 206–207).

Growth factors for the more-hygroscopic particles averaged over the European pollution outbreak time periods are given in Tables 8–10. As seen from Tables 5–10 and Figs. 1, 2, the average growth factors for the more-hygroscopic particles are only slightly lower in the European plume than in clean marine air masses.

5.3. *Local pollution*

Freshly produced aerosol particles caused by local anthropogenic pollution are likely to have hygroscopic properties which are markedly different from those of aged particles. Combustion of fossil fuels, e.g., in gasoline and diesel powered vehicles, produce large numbers of nearly hydrophobic particles in the size range from about 10 to a few hundred nm (Weingartner et al., 1997). The properties of recently emitted particles of anthropogenic origin can be studied using H-TDMA data for time periods when local pollution was suspected. At Hidalgo, this was based of wind direction, wind speed and particle concentration (see Section 2), and summarised as the time fraction, f, of every 10-min period when sampling was in the clean sector. The selection of H-TDMA scans with probable local pollution was done by taking only the 10–minute periods for which the clean sector criteria were never fulfilled ($f = 0$). It should be noted that some of the local pollution events were taken out of the Hidalgo H-TDMA data set due to the stability criteria. Furthermore, 10-min periods for which $f = 0$ can also be caused simply by low wind speeds (< 1 m s^{-1}).

As seen in Table 11, the frequency of occurrence of near-hydrophobic particles (22–49%) is distinctly higher during periods of local pollution ($f = 0$) than in both clean marine (Table 5) and European outbreak air masses (Table 8), for which the frequencies are $< 3\%$ and $< 1\%$, respectively.

Table 4. *Time periods selected as European plume outbreaks (1 January 1997 at noon is DOY = 1.5) at the various MBL sites*

European plume outbreaks					
Hidalgo		Sagres		ship	
day of Year	start date	day of year	start date	day of year	start date
187.46–192.15	6 July	185.9–186	4 July	189.2–189.7	8 July
198.12–200.52	17 July	186.5–189	5 July	190.5–192.5	9 July
205.71–208.0	24 July	199–202	18 July	202–203.8	21 July

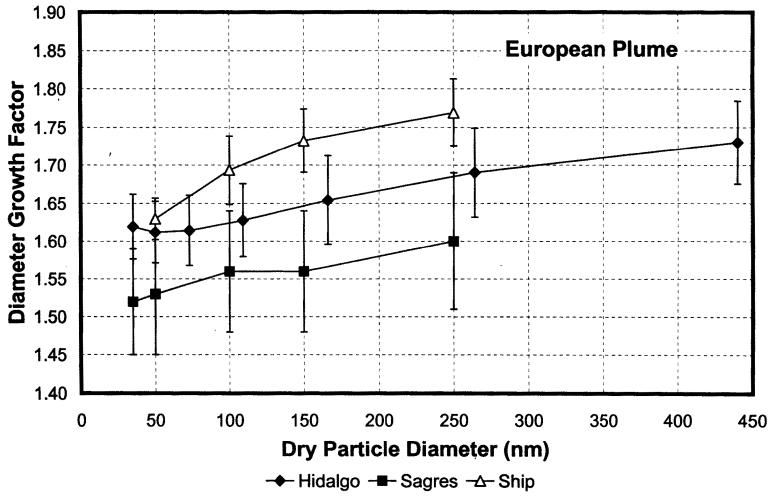

Fig. 2. Hygroscopic diameter growth factor averages ± one standard deviation (at RH = 90%) for the European plume outbreaks at Hidalgo (Tenerife), Sagres (Portugal) and the ship.

Overall, the frequency of occurrence of near-hydrophobic particles is highest for particles <110 nm, as expected from combustion sources. The frequency is also higher for $f = 0$ (36% including all sizes) than for any interval of 0.1 in f with $f > 0$ (2–23%), with a trend of decreasing frequency for increasing values of f. A similar trend can not be seen for the less-hygroscopic particles, for which the frequency of occurrence is fairly constant (0–9%) over all intervals of f, indicating that at Hidalgo these particles do not originate from local pollution sources (see discussion below regarding free tropospheric growth factors).

In conclusion, sources of local pollution, most likely combustion, produce near-hydrophobic particles. These particles are observed very rarely in aged air masses free from local pollution. It is not likely that the deposition velocity of the near-hydrophobic particles is higher than for particles that are more hygroscopic. The scarcity of such particles in aged air masses is therefore indicative of atmospheric processes adding water-soluble material during transport away from the sources.

5.4. *Free troposphere*

As discussed in Russell et al. (1998), the structure of the marine lower troposphere can not be adequately described using the classical conception of a well-mixed turbulent lower boundary layer (BL) capped by an inversion defining the transition to a stable FT aloft. Over land, cloud venting frequently causes air to penetrate the capping inversion and spill BL air into the FT, resulting in a transition layer between the BL and the FT. Rising of the capping inversion during daytime and sinking at night also contribute to the creation of a transition layer. Even though both cloud convection and diurnal effects are less pronounced over the ocean than over land, a similar transition layer, or buffer layer, may develop also in the marine troposphere (Russell et al., 1998; Johnson et al., 2000; Sollazzo, et al., 2000). The turbulence in the buffer layer is less consistent than in the well-mixed MBL, and caused both by wind shear and cumulus convection penetrating from the MBL. Due to the intermittent turbulence, some vertical layering of the buffer layer may appear. The buffer layer is capped by an inversion that defines the transition to the stably stratified FT. In the ACE-2 region, the capping inversion is strengthened by large-scale subsidence around the Azores high-pressure system. Scattered cumulus or stratocumulus clouds often appear at the top of the well-mixed, turbulent lower MBL. Additional cloud layers may also form in the buffer layer or at the FT inversion.

Radiosonde vertical profiles taken at Punta del Hidalgo during the ACE-2 campaign show that,

Table 5. *A summary of the H-TDMA observations made in clean marine air masses at Punta del Hidalgo on Tenerife during the ACE-2 experiment, 16 June to 25 July 1997*

	Dry particle diameter							
Growth at 90% RH	35 nm	50 nm	73 nm	109 nm	166 nm	264 nm	440 nm	All sizes
Total number of observations	97	110	110	120	112	110	24	683
More-hygroscopic particles								
growth factor (average ± 1 s.d.)	1.65 ± 0.05	1.64 ± 0.04	1.65 ± 0.05	1.67 ± 0.04	1.71 ± 0.05	1.74 ± 0.05	1.76 ± 0.06	
frequency of occurrence	100%	100%	100%	100%	100%	100%	100%	($n = 683$)
number fraction (when present)	1.00 ± 0.03	0.99 ± 0.06	0.99 ± 0.05	0.99 ± 0.04	0.99 ± 0.05	0.96 ± 0.10	1.00 ± 0.00	
"Hydrophobic" particles								
growth factor (average ± 1 s.d.)	1.05 ± 0.01	1.06 ± 0.02	1.04 ± 0.04	1.03 ± 0.03		1.00 ±		
frequency of occurrence	3.1%	2.7%	1.8%	2.5%	0%	0%	0%	($n = 12$)
number fraction (when present)	0.15 ± 0.12	0.24 ± 0.18	0.25 ± 0.25	0.16 ± 0.12		0.14 ±		
Less-hygroscopic particles								
growth factor (average ± 1 s.d.)		1.33 ± 0.01	1.35 ±	1.35 ± 0.03	1.34 ± 0.02	1.33 ± 0.03		
frequency of occurrence	0%	1.8%	0.9%	2.5%	7.1%	13.6%	0%	($n = 29$)
number fraction (when present)		0.23 ± 0.10	0.29 ±	0.14 ± 0.00	0.18 ± 0.07	0.28 ± 0.08		

The results are expressed as average hygroscopic growth factors (defined as the particle diameter at RH = 90% divided by the diameter at RH < 10%) for the various externally mixed particle groups showing different hygroscopic properties. Frequency of occurrence refers to the relative number of H-TDMA scans for which the hygroscopic mode in question was detected. Number fraction is a measure of the relative number of particles assigned to the particular mode when present. The selected time periods are DOY 167, 169, 171, 173–179, 183–186, 193–197, 204–205.

Table 6. *Same as Table 5, but for Sagres (Portugal), clean marine air masses*

Growth at 90% RH	Dry particle diameter					
	35 nm	50 nm	100 nm	150 nm	250 nm	All sizes
Total number of observations	61	61	62	65	65	314
More-hygroscopic particles						
growth factor (average ± 1 s.d.)	1.54 ± 0.07	1.55 ± 0.07	1.60 ± 0.08	1.65 ± 0.09	1.65 ± 0.07	
frequency of occurrence	100%	100%	100%	100%	100%	($n = 314$)
number fraction (when present)	0.98 ± 0.09	0.99 ± 0.06	0.96 ± 0.15	0.98 ± 0.06	0.99 ± 0.06	
Less-hygroscopic particles						
growth factor (average ± 1 s.d.)	1.16 ± 0.07	1.20 ± 0.11	1.14 ± 0.09	1.20 ± 0.15	1.23 ± 0.13	
frequency of occurrence	11.5%	8.2%	22.6%	12.3%	9.2%	($n = 40$)
number fraction (when present)	0.21 ± 0.19	0.18 ± 0.11	0.18 ± 0.27	0.13 ± 0.11	0.14 ± 0.13	

The selected time periods are DOY 172.83–173.50, 177.50–178.40, 179.10–179.80, 180.00–181.20, 184.00–185.00.

Table 7. *Same as Table 5, but for the ship R/V Vodyanitsky, clean marine air masses*

Growth at 90% RH	Dry particle diameter				
	50 nm	100 nm	150 nm	250 nm	All sizes
Total number of observations	104	107	115	119	445
More-hygroscopic particles					
growth factor (average ± 1 s.d.)	1.64 ± 0.04	1.73 ± 0.04	1.77 ± 0.04	1.80 ± 0.04	
frequency of occurrence	100%	100%	100%	100%	($n = 445$)
number fraction (when present)	1.00 ± 0.00	1.00 ± 0.01	1.00 ± 0.02	1.00 ± 0.01	
Less-hygroscopic particles					
growth factor (average ± 1 s.d.)		1.04 ± 0.01	1.02 ±	1.03 ±	
frequency of occurrence	0%	1.9%	0.9%	0.9%	($n = 4$)
number fraction (when present)		0.08 ± 0.02	0.17 ±	0.10 ±	

The selected time periods are DOY 173.5–174.7, 177.5–181.5, 183.5, 186.2, 192.5–193.5, 201.2–202.

at least from a thermodynamic point of view, the Izaña observatory (2367 m asl) is often found to be at the top of the buffer layer during night-time, and not in the FT. The air measured at the Izaña site is therefore a mixture of MBL and FT air, the exact proportions of which vary over time. Keeping this in mind, the term FT will be used to incorporate both FT and buffer layer air in the discussion below.

During daytime hours, the air at Izaña is clearly affected by MBL air and local emissions (anthropogenic or biogenic) due to up-slope winds. During the night-time, the air mass is more representative of FT air (with the reservations made above). An attempt was made to separate the available H-TDMA data into these two types of conditions (FT versus MBL influence).

For most of the time, the H-TDMA measurements at the Izaña observatory were performed at 10 nm dry particle size in order to investigate the composition of the ultrafine mode particles during possible nucleation events under free tropospheric conditions. In addition, particles with 50 nm dry size were studied during several days for comparison with the H-TDMA measurements in the MBL.

Table 8. *Same as Table 5, but for Punta del Hidalgo (Tenerife), European outbreak air masses*

Growth at 90% RH	Dry particle diameter							
	35 nm	50 nm	73 nm	109 nm	166 nm	264 nm	440 nm	All sizes
Total number of observations	93	97	99	89	97	87	80	642
More-hygroscopic particles								
growth factor (average $\pm$ 1 s.d.)	1.62 ± 0.04	1.61 ± 0.04	1.61 ± 0.05	1.63 ± 0.05	1.65 ± 0.06	1.69 ± 0.06	1.73 ± 0.05	
frequency of occurrence	100%	100%	100%	100%	100%	100%	100%	($n = 993$)
number fraction (when present)	0.99 ± 0.04	1.00 ± 0.00	1.00 ± 0.03	1.00 ± 0.00	1.00 ± 0.00	1.00 ± 0.00	1.00 ± 0.00	
"Hydrophobic" particles								
growth factor (average $\pm$ 1 s.d.)	$1.05 \pm$		$1.11 \pm$					
frequency of occurrence	1.1%	0%	1.0%	0%	0%	0%	0%	($n = 2$)
number fraction (when present)	$0.29 \pm$		$0.14 \pm$					
Less-hygroscopic particles								
growth factor (average $\pm$ 1 s.d.)	1.34 ± 0.13		1.32 ± 0.12					
frequency of occurrence	2.2%	0%	2.0%	0%	0%	0%	0%	($n = 4$)
number fraction (when present)	0.17 ± 0.09		0.16 ± 0.02					

The selected time periods are DOY: 187.46–192.15, 198.12–200.52, 205.71–208.0.

Table 9. *Same as Table 5, but for Sagres (Portugal), European outbreak air masses*

	Dry particle diameter					
Growth at 90% RH	35 nm	50 nm	100 nm	150 nm	250 nm	All sizes
Total number of observations	147	147	148	148	143	733
More-hygroscopic particles						
growth factor (average ± 1 s.d.)	1.52 ± 0.07	1.53 ± 0.08	1.56 ± 0.08	1.56 ± 0.08	1.60 ± 0.09	
frequency of occurrence	100%	100%	100%	100%	100%	($n = 733$)
number fraction (when present)	0.91 ± 0.18	0.97 ± 0.09	0.99 ± 0.04	0.99 ± 0.04	0.86 ± 0.15	
Less-hygroscopic particles						
growth factor (average ± 1 s.d.)	1.17 ± 0.06	1.13 ± 0.06	1.14 ± 0.07	1.18 ± 0.08	1.20 ± 0.06	
frequency of occurrence	34.7%	20.4%	7.4%	15.5%	63.6%	($n = 206$)
number fraction (when present)	0.34 ± 0.29	0.16 ± 0.15	0.14 ± 0.08	0.09 ± 0.06	0.24 ± 0.15	

The selected time periods are DOY: 185.9–186, 186.5–189, 199–202.

Table 10. *Same as for Table 5, but for the ship R/V Vodyanitsky, European outbreak air masses*

	Dry particle diameter				
Growth at 90% RH	50 nm	100 nm	150 nm	250 nm	All sizes
Total number of observations	40	31	46	47	164
More-hygroscopic particles					
growth factor (average ± 1 s.d.)	1.63 ± 0.03	1.69 ± 0.05	1.73 ± 0.04	1.77 ± 0.04	
frequency of occurrence	100%	100%	100%	100%	($n = 164$)
number fraction (when present)	0.99 ± 0.03	1.00 ± 0.00	1.00 ± 0.01	1.00 ± 0.02	
Less-hygroscopic particles					
growth factor (average ± 1 s.d.)	1.08 ± 0.04		1.06 ±	1.10 ±	
frequency of occurrence	5.0%	0%	2.2%	2.1%	($n = 4$)
number fraction (when present)	0.11 ± 0.05		0.06 ±	0.11 ±	

The selected time periods are DOY: 189.2–189.7, 190.5–192.5, 202–203.8.

5.4.1. Data for 10 nm particles. The hygroscopic properties of the nucleation mode particles were examined by measuring the hygroscopic growth distribution of 10 nm dry particles and correcting the results to RH = 90%. The general pattern was that a nucleation mode was present predominantly during daytime and therefore night-time data is rather sparse.

The total volume of 3–800 nm (dry size) particles calculated from the integral of the Izaña DMPS number size distribution was used to select time periods for which there was no or very little contamination of the FT air from sources in the MBL. An upper limit of 0.5 $\mu m^3\ cm^{-3}$ was chosen to select the unpolluted cases. The total particle concentration could not be used as an indicator of pollution since the purpose of the measurements at 10 nm was to study new particle formation events in FT air masses. Furthermore, trace gas data which could have been used for selecting unpolluted FT time periods (e.g., NO and CO) was not available.

Again, it should be emphasised that the air measured at the Izaña site is often within the buffer layer, and that therefore the conclusions drawn here are valid for FT air with minimal, but possible, influence from MBL sources.

A summary of the observations is given in Table 13. The following conclusions regarding the 10 nm particles in FT air masses can be made.

1. The particles were internally mixed, at least

Table 11. *Same as Table 5, but for Punta del Hidalgo (Tenerife) during incidents of local pollution*

Growth at 90% RH	Dry particle diameter							
	35 nm	50 nm	73 nm	109 nm	166 nm	264 nm	440 nm	All sizes
Total number of observations	79	84	84	81	85	77	25	515
More-hygroscopic particles								
growth factor (average ± 1 s.d.)	1.61 ± 0.11	1.63 ± 0.09	1.64 ± 0.06	1.67 ± 0.04	1.71 ± 0.05	1.75 ± 0.05	1.81 ± 0.07	
frequency of occurrence	100%	100%	100%	100%	100%	100%	100%	($n = 515$)
number fraction (when present)	0.78 ± 0.29	0.83 ± 0.26	0.81 ± 0.24	0.88 ± 0.16	0.94 ± 0.10	0.95 ± 0.09	1.00 ± 0.00	
"Hydrophobic" particles								
growth factor (average ± 1 s.d.)	1.08 ± 0.03	1.07 ± 0.04	1.06 ± 0.04	1.05 ± 0.04	1.04 ± 0.03	1.02 ± 0.02		
frequency of occurrence	40.5%	35.7%	41.7%	49.4%	36.5%	22.1%	0%	($n = 185$)
number fraction (when present)	0.40 ± 0.23	0.33 ± 0.22	0.35 ± 0.20	0.22 ± 0.16	0.16 ± 0.09	0.15 ± 0.05		
Less-hygroscopic particles								
growth factor (average ± 1 s.d.)	1.29 ± 0.06	1.30 ± 0.07	1.32 ± 0.10	1.38 ± 0.11	1.37 ± 0.02	1.47 ± 0.04		
frequency of occurrence	12.7%	10.7%	9.5%	3.7%	3.5%	2.6%	0%	($n = 35$)
number fraction (when present)	0.41 ± 0.23	0.50 ± 0.32	0.45 ± 0.23	0.29 ± 0.08	0.17 ± 0.14	0.22 ± 0.05		
Sea spray particles								
growth factor (average ± 1 s.d.)	2.08 ± 0.03	2.11 ±	2.10 ± 0.07	2.11 ±		2.16 ±		
frequency of occurrence	3.8%	1.2%	3.6%	1.2%	0%	1.3%	0%	($n = 9$)
number fraction (when present)	0.11 ± 0.03	0.12 ±	0.14 ± 0.07	0.18		0.51 ±		

regarding their hygroscopic properties (an external mixture was observed in only 1% of the measurements).
2. The particles were almost hydrophobic (96% of all observations).
3. On a few occasions higher growth factors were observed. These were related to North Atlantic air masses and probably indicate the presence of sulphate compounds in the nucleation mode particles.

The 10 nm or ultrafine particles observed in the FT at night were much less hygroscopic than would be expected of condensed species such as sulphuric acid or even some organic acids. This is in sharp contrast to observations at larger sizes both at Izaña and elsewhere on Tenerife and other sites during the ACE-2 campaign. The chemical composition of these particles is unknown. Even though the low growth factors indicate that sulphur compounds were not the main constituents of the 10 nm particles, it is still quite possible that these particles were formed by homogeneous binary nucleation of sulphuric acid–water vapour or ternary nucleation of sulphuric acid–water vapour–ammonia, followed by condensational growth caused by organic compounds. The forest growing on the slopes below Izaña is a possible source of organic precursors, such as monoterpenes.

5.4.2. Data for 50 nm particles. For the periods 18–19 June and 18–25 July 1997, 50 nm particles were investigated. A summary of the observations is given in Table 13. The following general conclusions can be made.

1. An external mixture was observed with typically three separate groups of particles identified by different modes in the hygroscopic growth distribution.
2. The less-hygroscopic particles were most frequent, followed by the more-hygroscopic particles.
3. A bimodal growth distribution was observed in 47% of the selected cases (i.e., polluted cases excluded).

For further analysis of the 50 nm growth data, periods of FT air were selected using three criteria: (i) total aerosol volume $<0.5\ \mu m^3\ cm^{-3}$; (ii) total particle concentration $<600\ cm^{-3}$; and (iii) night-time data only between 00:00 and 06:00 h. The particle group showing the lowest growth factor (~ 1.15) was most likely caused by local emissions, since it disappeared almost completely when all selection criteria mentioned above were applied. This is in contrast to the persistent appearance of the near-hydrophobic 10 nm particles. The other two particle groups with higher growth factors remained in the selected FT data set, with the less-hygroscopic particles (growth factor ~ 1.40) dominating in concentration (average 75% of aerosol number fraction).

An attempt was also made to study the dependence of the FT hygroscopic growth factors according to air mass history. The analysis was complicated by the fact that air mass back trajectories were only available for arrival at Izaña at 12:00 local time, while most of the FT data was obtained during night-time. In addition, most of the time when the air masses originated from the North Atlantic, the trajectories were rather close to the Portuguese coast making it difficult to completely rule out a European continental influence. The average less- and more-hygroscopic growth factors for 50 nm particles in FT air masses of predominantly European, North American and North Atlantic origin were quite similar, and within ± 1 standard deviation around the mean. Considering the difficulties in determining the air mass origin, no further conclusions could be drawn.

6. Discussion

6.1. Clean marine background air masses

As seen in Fig. 1 and Tables 5–7, there is a significant difference between the growth factors of the more-hygroscopic particles at the various sites when averaged over the clean marine periods. While the highest growth factors were observed on the ship, substantially lower values were measured at Sagres than at both Hidalgo and on the ship. These discrepancies should be explainable in terms of the chemical composition of the individual aerosol particles sampled at the various sites. In general, one would expect to observe low growth factors during periods with high pollution levels and high crustal influence, while a high relative sea-salt contribution would result in elevated growth factors. Useful tracers for anthropogenic pollution that were also available are particle

concentration, soot (aerosol absorption) and SO_2. Furthermore, soot gives a direct indication as to how much water-insoluble mass is present in the aerosol particles. Sodium (Na^+), being one of the major ions in sea-water and distributed predominantly in the atmospheric particulate phase, serves as an excellent tracer for sea-salt.

Since the hygroscopic growth factors were only measured for particles < 440 nm (expressed as equivalent mobility diameter at a dehydrated state), only the sub-micrometer particles are of interest here. The impactor data available and relevant for this study are (expressed as equivalent aerodynamic diameter), for Sagres ($D_{ae} < 0.14$ μm and $0.14\ \mu m < D_{ae} < 0.42\ \mu m$ at RH = 60%; Neusüß et al., 2000), for Hidalgo ($D_{ae} < 0.45$ μm at RH = 50%), and for the ship ($D_{ae} < 0.18$ μm and $0.18\ \mu m < D_{ae} < 0.31\ \mu m$ at RH = 55%; Quinn et al., 2000).

A full comparison of measured and modelled hygroscopic growth factors (a hygroscopic closure study) is beyond the scope of this paper and will be the topic of future publications. Furthermore, it is desirable to attempt to explain the hygroscopic behaviour on the basis of some rather simple parameters that can be either accurately measured or modelled with some confidence. The ultimate aim of such an exercise would be to implement these parameterisations in regional or global models in order to estimate hygroscopic growth factors over larger spatial and temporal scales.

Consider first the sea-salt influence on the observed hygroscopic growth factors. Mixtures of NaCl and Na_2SO_4 show a gradual decrease in growth factors from 2.4 (at RH = 90% for particles with dry diameters $>$ ca. 200 nm) for pure NaCl to 1.9 for pure Na_2SO_4 based on data from Tang (1997). As a result, a corresponding decrease in growth factors is expected as freshly produced sea-salt particles add secondary sulphate mass, derived either from biogenic DMS or from anthropogenic SO_2. The $Na^+/SO_4^=$ molar ratio, being a simple measure of the relative influence of sea-salt versus secondary sulphate, can therefore be expected to manifest itself in the hygroscopic growth factors, provided that sodium and sulphate exist in an internal mixture.

In-situ laser mass spectrometry measurements of the chemical composition of individual aerosol particles were performed at Cape Grim, Tasmania during the ACE-1 experiment in November–December 1995 (Murphy et al., 1998). For the unpolluted cases, more than 90% of the particles larger than the lower limit of the instrument (0.16 μm in diameter) contained sea-salt. Most of the sulphur was internally mixed with sodium in the individual particles, indicating that sodium sulphate is a common constituent, not only of the bulk MBL aerosol, but also of the single particles.

Concurrently during the ACE-1 experiment, ship-based H-TDMA measurements were performed in the Southern Ocean (Berg et al., 1998). Here, the presence of externally mixed sea-salt particles was evident at wind speeds $>$ ca. 10 m s^{-1}. These freshly produced sea-salt particles, with growth factors (dry to RH = 90%) between 2.0–2.3 similar to that of pure NaCl, were observed in 40% of all scans for 150 nm dry size particles, and could be found as far down in size as 50 nm. Once the wind speed decreased, the sea-salt particles were no longer observable as an external mixture since they were most likely transformed into more-hygroscopic particles by fixation of sulphate within a time frame of a few hours. However, the correlation between local wind speed and externally mixed sea-salt particle concentrations was poor.

The upward sea-salt particle flux is strongly dependent on wind speed (Nilsson et al., 1998). Even though sea-salt particle concentrations are the result of this upward flux balanced by appropriate downward fluxes (i.e., sinks) and integrated over the air mass back trajectory, local wind speed can nevertheless serve as a rough indicator of the relative sea-salt influence. Attempts to relate local wind speed directly to sea-salt particle concentrations have sometimes been successful (O'Dowd and Smith, 1993), and sometimes not (Berg et al., 1998).

As seen from Table 12, the $Na^+/SO_4^=$ molar ratios for the clean marine air masses indicate a higher relative influence of sea-salt at the ship than for both Sagres and Hidalgo. The higher overall wind speeds at the ship compared to Sagres and Hidalgo can at least partly account for the higher growth factors observed on the ship relative to Sagres and Hidalgo. For comparison, the average wind speed at the ship R/V Discoverer during the ACE-1 intensive campaign in the Southern Ocean was 9.5 ± 3.8 m s^{-1} (Bates et al., 1998), and resembled those at the R/V Vodyanitsky.

The conclusion is that, in the clean marine air

Table 12. *Summary of the average wind speed, $Na^+/SO_4^=$ molar ratio, soot and particle number (CN) concentrations, during the time periods of clean marine air and European outbreak air masses at Punta del Hidalgo (Tenerife), Sagres (Portugal) and the ship R/V Vodyanitsky; the upper particle sizes are given as equivalent aerodynamic diameters*

	Wind speed (ms^{-1})	$Na^+/SO_4^=$ molar ratio	Soot ($ng\,m^{-3}$)	CN (cm^{-3})
Clean marine air				
Sagres		0.15 (<0.42 μm)	40.0 ± 28.8	1660 ± 549
Hidalgo	6.5 ± 1.9	0.15 (<0.45 μm)	35.9 ± 37.2	462 ± 183
Ship	8.2 ± 2.8	0.51 (<0.31 μm)	19.4 ± 26.6	941 ± 558
European outbreaks				
Sagres		0.04 (<0.42 μm)	611 ± 232	7781 ± 2921
Hidalgo	6.6 ± 1.6	0.08 (<0.45 μm)	137.5 ± 62.0	1312 ± 722
Ship	11.1 ± 1.8	0.14 (<0.31 μm)	124 ± 75	1696 ± 547

Table 13. *Summary of the H-TDMA observations made at the Izaña observatory, Tenerife (2367 m asl) during the ACE-2 experiment, 16 June to 25 July 1997*

Growth at 90% RH	Dry particle diameter			
	10 nm	10 nm "clean"	50 nm	50 nm "clean"
Total number of observations	732	421	869	537
time period	17 June–19 July 1997 23 July 1997		18–19 June 1997 18–25 July 1997	
More-hygroscopic particles				
growth factor (average ± 1 s.d.)	1.28 ± 0.04	1.24 ± 0.06	1.61 ± 0.09	1.62 ± 0.06
frequency of occurrence	3%	4%	49%	54%
number fraction (when present)	1.5%	2.0%	12.9%	24.7%
"Hydrophobic" particles				
growth factor (average ± 1 s.d.)	1.05 ± 0.04	1.05 ± 0.03	1.14 ± 0.03	
frequency of occurrence	97%	96%	26%	
number fraction (when present)	98.2%	98.0%	15.2%	
Less-hygroscopic particles				
growth factor (average ± 1 s.d.)			1.40 ± 0.05	1.43 ± 0.06
frequency of occurrence			76%	71%
number fraction (when present)			56.1%	75.3%

The results are expressed as average hygroscopic growth factors (defined as the particle diameter at RH = 90 % divided by the diameter at RH < 10%) for the various externally mixed particle groups showing different hygroscopic properties. The clean periods were selected as follows: For 10 nm particles; all periods when the aerosol particle volume integrated from DMPS measurements was $<0.5\,\mu m^3\,cm^{-3}$. For 50 nm particles; night time data (00–06) and CN concentrations $<600\,cm^{-3}$ and particle volume $<0.5\,\mu m^3\,cm^{-3}$.

masses for which sea-spray is the dominating source of primary aerosol particles, higher overall wind speeds result in a larger production of sea-salt particles and thus also particles with a higher $Na^+/SO_4^=$ molar ratio and higher hygroscopic growth factors.

As seen in Fig. 1, the more-hygroscopic growth factors measured at Sagres during the clean marine cases are significantly lower than at both Hidalgo and on the ship. A very conservative selection was made of the time periods when the Sagres site was believed to have experienced minor influence from pollution sources. However, there were only very short glimpses of what might have been clean

marine air at Sagres during the ACE-2 period, and even these were probably affected by anthropogenic sources. The elevated particle concentrations indicate possible contamination (Table 12). Also other trace gases were found at higher concentrations than can be expected in truly remote marine environments (SO_2: 0.37 ± 0.20 ppb; CO: 14.4 ± 24.7 ppm; NO: 0.21 ± 0.12 ppb; NO_2: 0.75 ± 0.36 ppb; O_3: 27.4 ± 3.9 ppb).

6.2. *Continental influence — European outbreaks*

As noted already, the average growth factors for the more-hygroscopic particles are only slightly lower in the European plume than in clean marine air masses. The site-to-site differences are in fact larger than that attributable to air mass history. Indeed, at each of the sites, the growth factors of the more-hygroscopic particles are quite similar for the 35 and 50 nm dry sizes in both these air masses, with the largest differences in the particle size range 100–166 nm. The low $Na^+/SO_4^=$ molar ratio in combination with the high soot and particle concentrations during the European outbreaks (Table 12) would otherwise suggest rather low growth factors, especially for the Sagres site. As already pointed out, the Sagres growth factors were quite low even for the clean marine cases, probably due to the difficulties in selecting truly marine air masses at this continental site.

The most striking feature of the European plume as it reaches the ship and Hidalgo is the near absence of particles with low growth factors ($<$ca. 1.4–1.5), i.e., particles classified as near-hydrophobic or less-hygroscopic (Tables 8, 10). This is in sharp contrast to the hygroscopic properties of particles in the well-mixed, but considerably fresher plume as it leaves the European continent at Sagres (Table 9). Here, the frequency of occurrence of less-hygroscopic 250 nm particles was as high as 64%, with an average number fraction of 24% when present.

During the Sagres European outbreak periods, there was a general temporal pattern. As the Sagres site came into the plume, the more-hygroscopic growth factors decreased while the less-hygroscopic growth factors increased and the number fraction of less-hygroscopic particles increased concurrently. In the very centre of the plume, the more- and less-hygroscopic growth factors tended to merge at an intermediate value (around 1.3), resulting in an internal hygroscopic mixture. The opposite was taking place as Sagres came out of the plume again, i.e., the more-hygroscopic growth factors increased, the less-hygroscopic growth factors decreased and the number fraction less-hygroscopic particles decreased. These quantities finally reached the values they had before entering the plume. This pattern was most pronounced for the 250 nm particles.

Apparently, less-hygroscopic particles accrete water-soluble material in the ageing plume and finally become indistinguishable from the more-hygroscopic particles. In other words, the externally mixed aerosol evolves into an internal one, at least from a hygroscopic point of view. Processes that are likely candidates for this transformation are coagulation, condensation and cloud-processing, of which the two latter are probably dominant (Bates et al., 2000; Hoell et al., 2000; Raes et al., 2000; Kerminen, 1997).

Cloud-processing includes dissolution of water-soluble gases followed by fixation in the particulate phase, scavening of unactivated interstitial aerosol particles by cloud droplets and droplet coalescence. Subsequent droplet evaporation will then preferentially yield more-hygroscopic particles. It should be noted that even though the H-TDMA observes an internal mixture, the particles at a given dry size may still be externally mixed from a chemical point of view.

6.3. *FT-MBL vertical mixing*

Even though it is not the purpose of this paper to draw any definite conclusions regarding the FT-MBL vertical mixing, the Tenerife 50 nm H-TDMA data nevertheless provide some insights in this matter. Since the more-hygroscopic mode totally dominates in the MBL, while the less-hygroscopic mode is the most frequent in the FT, particles not belonging to the dominant mode of each layer can possibly be the result of FT-MBL mixing.

A direct FT-MBL intercomparison of the hygroscopic properties of 50 nm particles could be made for the two time periods when the Izaña H-TDMA was set to operate at this particle size, 18–19 June and 18–25 July 1997. The June period shows excellent agreement for the more-hygroscopic growth factors, suggesting that MBL air near sea

level (Hidalgo, 63 m asl) had mixed up to the altitude of Izaña (2367 m asl). For the July period, there were also occasions with good agreement between the FT and MBL sites for the more-hygroscopic particles, but these are of rather short duration. Indeed, there were times when there was no resemblance whatsoever between the hygroscopic growth factors measured in the FT and MBL, indicating insignificant FT-MBL mixing. An example of this occurred for almost the entire 24 July, when all 50 nm particles at Izaña had growth factors of 1.3–1.4, while the corresponding MBL values were stable around 1.55–1.6 with no signs of less-hygroscopic particles.

In the early morning hours of 20 July, less-hygroscopic particles (growth factors of 1.3–1.5) appeared at Hidalgo in the Aitken mode (35, 50 and 73 nm dry sizes). Air mass back trajectories ending over Hidalgo at noon on 19 and 20 July at the 975 hPa level crossed the 900 hPa level down into the MBL 48 h before reaching Tenerife, and had subsided from ca. 700 hPa 5 days previously. During the event on 20 July, the wind shear caused by elevated wind speeds in the layer immediately above the MBL is likely to have favoured entrainment across an otherwise very strong and narrow temperature inversion.

Since, in the selected FT data set, the less-hygroscopic particles (growth factors $\sim$1.40) constitute on average 75% of the aerosol number fraction, it might be hypothesised that the occurrence of less-hygroscopic particles in the MBL at Hidalgo is a direct observation of entrainment of FT air into the MBL. In the entire Hidalgo data set, the frequency of occurrence of less-hygroscopic particles varied with particle dry size between 0.5–6%. If the presence of less-hygroscopic particles at Hidalgo are indeed signs of entrainment of FT air, there might be various reasons why such less-hygroscopic particles were not observed other than intermittently in the MBL (63 m asl).

Entrainment of FT air into the MBL may have been sporadic and discontinuous, or the entrainment rate may have varied considerably in strength over time (Raes et al., 1997). The mixing time of the boundary layer is typically 1 h or less (Stull, 1988). Even if entrainment were a more or less continuous process, although of variable strength, the entrained particles might not be directly observable close to the sea surface. In other words, the entrained particles might lose the observable properties that make them uniquely identifiable as originating from the FT, such as their less-hygroscopic behaviour, before they reach the sea surface. This transformation would then have to be of the same order as the MBL mixing time, i.e., ca. 1 h. One likely process is passage through a stratocumulus cloud deck and concurrent fixation of soluble trace gases (e.g., SO_2), resulting in a more soluble particle with growth factors resembling those of the more-hygroscopic MBL particles.

7. Growth factor parameterisation

The aerosol mass concentration in the coarse and accumulation modes is the parameter of primary importance in determining the direct climate forcing by aerosols. The increase of aerosol mass as a result of water uptake due to variations in ambient RH is probably the second most important parameter (Plinis et al., 1995). Models describing the impact of atmospheric aerosols on the radiative balance therefore need to calculate particle size distributions as a function of a broad range of RH as occurs in the atmosphere.

Both measurement and modelling approaches can be used to determine the hygroscopic growth factor as a function of RH. To measure the growth factors for a large number of RHs, both for increasing and decreasing RH so that possible RH hysteresis effects can be identified, is time-consuming when carried out for a number of dry particle sizes. Furthermore, the results will be compromised if changes in air mass history occur during the measurement.

Alternatively, the growth factors measured at a limited number of humidities (e.g., 10%, 60% and 90%) can be used with a suitable model of hygroscopic growth to predict growth factors at intermediate values of RH. The resulting loss in RH resolution is countered by time resolution and simplified H-TDMA operation. If the size dependent concentrations of the major inorganic ions are known for the aerosol, thermodynamic models can be used in conjunction with the growth measurements to calculate the water mass uptake as a function of RH (Clegg et al., 1998).

Similar to the growth factor correction procedure (Section 4), the first step would then be to calculate the water-soluble volume fraction (ε) of

the individual particles as a function of dry size based on the measured growth factor at a single RH, and to use this ε to estimate the hygroscopic growth at any other RH (Swietlicki et al., 1999). Otherwise an empirical model or a hybrid between the thermodynamic and empirical approaches may be used. Within well-mixed, aged air masses of similar origin, variations in hygroscopic growth factors can be expected to be small over limited time and size ranges. Average chemical composition of the aerosol particles over ca. 24 h and factor of two size increments can therefore be used to model the hygroscopic growth with reasonable accuracy. As will be shown for clean marine air masses, the H-TDMA growth measurements, and thus also modelled parameters, show very little temporal variation in hygroscopic growth factor for a specific site and dry particle size.

During ACE-2, at two of the MBL sites, Sagres and Hidalgo, measurements were performed at regular intervals at an intermediate DMA2 RH (60 or 70%) in addition to the nominal 90% RH. Thus, the hygroscopic growth was measured at three separate RHs, since it was further assumed that the separation of quasi-monodisperse particles in DMA1 (RH < 10–15%) represented a measurement of a unity growth factor at RH = 0%. A simple two-parameter function was used to describe the hygroscopic growth factor as a function of RH,

$$G(\mathrm{RH}) = 10^{c}(1 - \mathrm{RH})^{\gamma}$$

Here, the RH at subsaturation is given directly as the ratio between the actual and saturation water vapour pressure (values between 0–1) and not in %. The two parameters c and γ are determined by fitting the model to the data.

At Hidalgo, 1 h of measurements at RH = 70% were performed every 6th hour for 50 and 166 nm particle dry sizes, representative of Aitken and accumulation mode particles. The 2–3 scans at RH = 70% for each dry size were grouped with the previous and subsequent 5 h of observations at RH = 90%.

Both the 70% and 90% RH growth factor values for each such group of data were averaged and were subsequently used, in addition to the point $G(0\%) = 1$, to perform the two-parameter fit of $G(\mathrm{RH})$ described above. At Sagres, measurements at RH = 60% were made once a day only, but then for all dry particle sizes (35, 50, 100, 150 and 250 nm) and for both increasing and decreasing (from 80% to 60%) RH. The grouping and averaging of data was made in the same way as for Hidalgo.

An example of the parameterisation is displayed in Fig. 3 for 50-nm particles in clean marine air masses at Hidalgo. The numerical results of parameterisations for clean and polluted conditions at all available sizes for both sites are summarised as averages and standard deviations in Table 14. Note that the parameterisations given here are valid for the predominant more-hygroscopic particle mode, and not for the externally mixed sea-salt particle mode. The c values for the various fits are all insignificantly different from zero, so that the RH dependence could equally well be described by $G(\mathrm{RH}) = (1 - \mathrm{RH})^{\gamma}$.

As noted previously, the Sagres site was probably affected by anthropogenic pollution even during marine flow. Even under clean conditions they are at best representative of slightly polluted marine aerosol. The screened Hidalgo data, on the other hand, was largely unaffected by local pollution and can therefore be considered representative for clean marine air masses, at least for wind speeds for which the local sea-salt production is small (< ca. 8 m s^{-1}). The one-parameter RH dependence at Hidalgo (for $G(0\%) = 1$), is likely to be the best parameterisation for the clean marine air masses in the north-eastern Atlantic, again for moderate wind speeds. For comparison, the γ values for 150 nm particles for some common inorganic compounds are ammonium bisulphate: $\gamma = -0.261$; ammonium sulphate: $\gamma = -0.243$. Of these, ammonium bisulphate gives the best fit to the modelled growth based on empirical water activity data (Tang and Munkelwitz, 1994).

The γ parameters in Table 14 show a decrease with increasing particle size, at least up to 250 nm. This dependency might be used to construct $G(\mathrm{RH})$ for sizes other than those for which direct measurements were performed.

As seen in Fig. 3, a few growth factors at RH = 70% fall below both the fitted lines and the bulk of data points. This is an indication that, in clean marine air masses at Hidalgo, particles occasionally exhibit RH hysteresis. At Sagres, where measurements were performed for both increasing and decreasing RH, a small but reproducible hysteresis was observed in more polluted air masses. During ACE-1, RH hysteresis was only observed occasion-

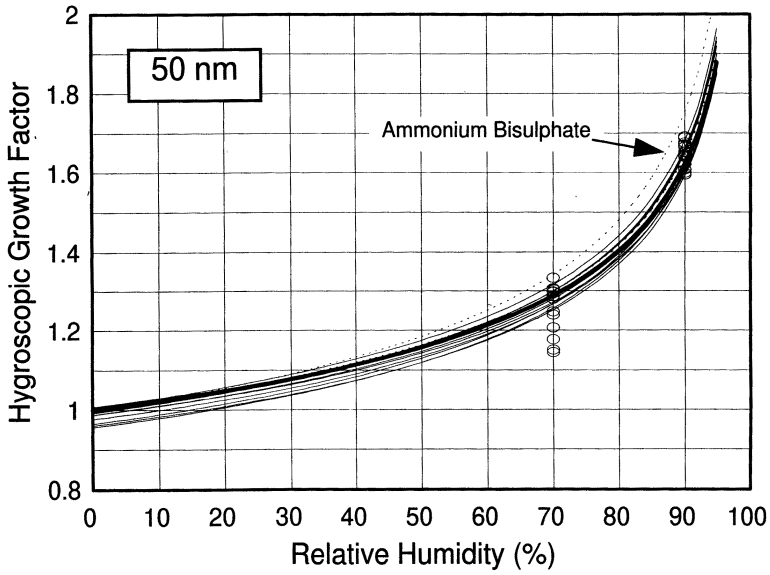

Fig. 3. Example of parameterisations of hygroscopic diameter growth factor versus RH for clean marine air masses at Hidalgo, Tenerife and 50 nm dry particle size. The thick line shows the averaged function $G(\mathrm{RH}) = (1 - \mathrm{RH})^{-0.210}$ while the thin lines depict the individual fits. Also given is the same type of parameterisation for ammonium bisulphate. Measured data points are shown as circles.

ally, and then only in the Pacific Ocean north of the South Pacific Gyre and for the Aitken mode particles (Berg et al, 1998). Particles of pure sodium chloride and ammonium sulphate deliquesce at 75 and 80% RH respectively.

This model is obviously limited in terms of its accuracy and applicability. First, it applies only to particles in the size range between 30 and 500 nm diameter, i.e., the accumulation and Aitken modes, and only to the general air mass types observed and categorised during ACE-2. Second, it applies only up to 90% RH. The parameterisation applies only to aerosols that are hygroscopic and not deliquescent and does not distinguish between the upper and lower bounds of the hysteresis effect that is possible between ca. 30% and 80% RH. Finally, the range of variability (Table 14) and the instrumental uncertainty (Table 2) must be considered and included in any application of this model.

8. Conclusions

The measurements of hygroscopic properties of sub-micrometer atmospheric aerosol particles in the subtropical north-eastern Atlantic during the second Aerosol Characterization Experiment (ACE-2) from 16 June to 25 July 1997 were carried out using the largest collection of Hygroscopic Tandem Differential Mobility Analysers (H-TDMA) participating in one single experiment to date. ACE-2 thus offered unique opportunities to study the transformation of hygroscopic properties of aerosol particles during transport from the source region (Europe) and over the Atlantic Ocean, as well as air mass mixing between the free troposphere and the marine boundary layer.

In clean marine BL air masses at Hidalgo and at the ship, a unimodal growth distribution of more-hygroscopic particles dominated, with growth factors ranging from 1.6 to 1.8 with a consistent increase in growth factor with increasing particle size. At Sagres, Portugal, less-hygroscopic particles with a growth factor of ca. 1.15 frequently occurred during polluted conditions. When this European plume had travelled over the ocean in the MBL to the ship and Hidalgo, particles with growth factors $<$ca. 1.4–1.5 were nearly absent. The less-hygroscopic particles were apparently modified by coagulation, condensation and cloud-processing during transport of the

Table 14. *Parameters c and γ fitted to the function $G(RH) = 10^{c}(1 - RH)^{\gamma}$ describing how hygroscopic growth factors vary with relative humidity RH (here expressed directly as a water vapour ratio and not in %)*

		Dry particle diameter					
Site	Parameter	35 nm	50 nm	100 nm	150 nm	166 nm	250 nm
Hidalgo	c	—	-0.005 ± 0.008	—	—	-0.002 ± 0.003	—
	γ	—	-0.216 ± 0.008	—	—	-0.235 ± 0.011	—
Hidalgo	γ, $G(0\%) = 1$	—	-0.210 ± 0.008	—	—	-0.233 ± 0.013	—
Sagres	c	-0.003 ± 0.006	-0.002 ± 0.004	-0.006 ± 0.006	-0.004 ± 0.006	—	-0.006 ± 0.005
	γ	-0.192 ± 0.017	-0.195 ± 0.017	-0.202 ± 0.019	-0.220 ± 0.016	—	-0.219 ± 0.011

The parameterisation is valid for the ubiquitous more-hygroscopic particles in clean marine air masses in the range $0 < RH < 0.90$. The one-parameter RH dependence at Hidalgo (for $G(0\%) = 1$), is likely to be the best parameterisation for the clean marine air masses in the north-eastern Atlantic, at least at wind speeds for which the local sea-salt production is small ($<$ ca. 8 ms^{-1}).

plume in the MBL to become indistinguishable from the more-hygroscopic particles (Fig. 4).

There is a significant difference between the growth factors of the more-hygroscopic particles at the various MBL sites when averaged over the clean marine periods. Indeed, the site-to-site differences are larger than that attributable to air mass history (clean marine or European outbreaks). Considering the careful quality assurance procedures to which the data was subjected, this site-dependence is not likely to be entirely caused by measurement inaccuracies. Instead, the differences can be explained by the chemical composition of the aerosol particles. For example, in the clean marine air masses for which sea-spray is the dominating source of primary aerosol particles, higher overall wind speeds result in a larger production of sea-salt particles and thus also particles with a higher $Na^{+}/SO_4^{=}$ molar ratio and higher hygroscopic growth factors.

For the first time, H-TDMA measurements were performed at a site (Izaña) which represents free tropospheric air with minimal, but possible, influence from MBL sources. The 10 nm particles observed at Izaña were internally mixed, at least regarding their hygroscopic properties, and almost hydrophobic. In contrast to this, the 50 nm particles showed an external mixture dominated by the less-hygroscopic particles with growth factors of about 1.4 (at RH = 90%). It seems that particles being transported in the FT are not converted to the more-hygroscopic state as fast as in the MBL. This is perhaps due to a lower frequency of cloud processing in the FT.

Climate modellers are encouraged to make full use of the extensive hygroscopic growth data set obtained during the ACE-2 experiment. The growth factor parameterisations should be of particular value in climate models incorporating the direct effect of aerosols on climate.

The growth factor parameterisations are only valid for RHs between 0–90% and particles in the size range 30–500 nm (dry size) that exhibit no RH hysteresis. The instrumental uncertainty and variation in growth factors for a given air mass type should be noted and included in any further applications.

Those measurements at Hidalgo and the ship which were classified as 'clean marine' are representative of aged marine air masses free of nearby anthropogenic influence and for moderate wind

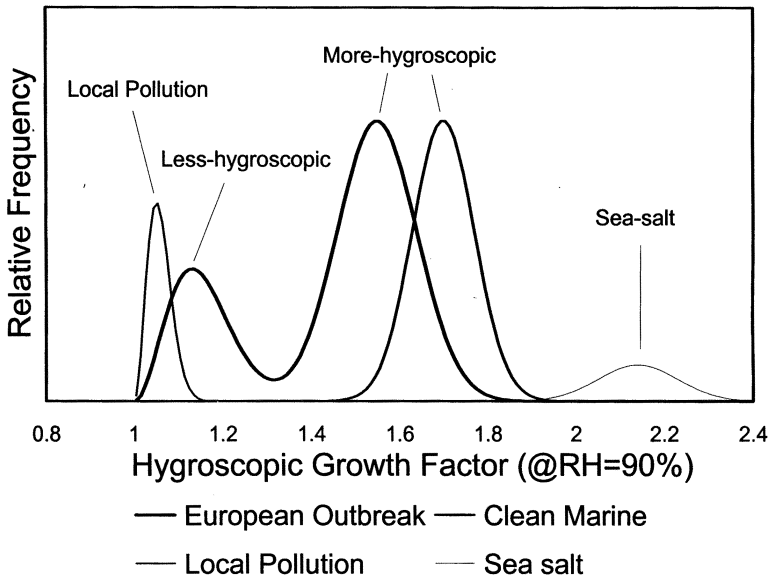

Fig. 4. Schematic diagram of the sub-micrometer particle hygroscopic behaviour observed in clean marine air masses at Hidalgo, Tenerife and in European plume outbreaks at Sagres, Portugal. The more-hygroscopic particle mode is always observed. Concentrations of particles originating from local pollution (combustion) and sea-spray vary considerably with time.

speeds typical of anticyclonic conditions. During these conditions, only the ubiquitous more-hygroscopic particle mode needs to be considered. At wind speeds higher than ca. 10 m s^{-1}, significant concentrations of externally mixed sea-salt particles will appear. The high growth factors of these freshly produced sea-salt particles (2–2.3 at RH = 90%) should then be taken into account by the climate models.

The Sagres site was probably affected by anthropogenic pollution of varying degree at all times. Even under clean conditions they are at best representative of slightly polluted marine aerosol. The data for the European outbreaks observed at Sagres could be used as starting point for models attempting to describe the evolution of aerosols in a well-mixed, anthropogenically influenced continental plume, the result of which could be gauged against the largely unimodal hygroscopic behaviour observed at the ship or at Hidalgo for air masses classified as European outbreaks, representative of well-aged polluted marine aerosols (Fig. 4).

Since the ACE-2 experiment was carried out in the summer, the emissions of DMS and its subsequent oxidation to produce sulphates is not likely to be representative of other times of the year. Thus, the transformation rate for sea-salt particles is dependent on season, which possibly also affects the growth factors.

The hygroscopic properties of Saharan dust outbreaks into the north-eastern Atlantic could not be adequately studied, since no such major dust event occurred during the ACE-2 campaign.

9. Acknowledgements

This research is a contribution to the International Global Atmospheric Chemistry (IGAC) Core Project of the International Geosphere–Biosphere Programme (IGBP) and is part of the IGAC Aerosol Characterization Experiments (ACE). DGXII of the European Commission supported the contributions from the universities in Lund and Helsinki under contracts ENV4-CT95-0140 (FREETROPE) and ENV4-CT95-0058 (HILLCLOUD), and the IfT contribution under contract ENV4–CT95–0108 (CLEARCOLUMN). Financial support for the measurements and analyses carried out by the University of Washington was provided by the

US National Science Foundation, ATM 9619984. This is University of Washington, JISAO contribution number 653. Lund University was also supported financially by the Swedish Environmental Protection Board and the Swedish Natural Science Research Council. University of Helsinki would also like to acknowledge the financial support from the Academy of Finland. We gratefully acknowledge the extensive logistic support by the Radio Naval station of Sagres, Portugal.

REFERENCES

Bates, T. S., Kapustin, V. N., Quinn, P. K., Covert, D. S., Coffman, D. J., Mari, C., Durkee, P. A., De Bruyn, W. J. and Saltzman, E. S. 1998. Processes controlling the distribution of aerosol particles in the lower marine boundary layer during the first Aerosol Characterization Experiment (ACE-1). *J. Geophys. Res.* **103**, 16369–16383.

Bates, T. S., P. K. Quinn, D. S. Covert, D. J. Coffman and D.W Johnson. 2000. Aerosol physical properties and controlling processes in the lower marine boundary layer: A comparison of sub-micron data from ACE-1 and ACE-2. *Tellus* **52B**, 258–272.

Berg, O. H., Swietlicki, E. and Krejci, R. 1998. Hygroscopic growth of aerosol particles in the marine boundary layer over the Pacific and Southern Oceans during ACE-1. *J. Geophys. Res.* **103**, 16535–16545.

Bower, K. N., Choularton, T. W., Gallagher, M. W., Beswick, K. M., Flynn, M., Allen, A. G., Davison, B. M., James, J. D., Robertson, L., Harrison, R. M., Hewitt, C. N., Cape, J. N., McFadyen, G. G., Martinsson, B. G., Frank, G., Swietlicki, E., Zhou, J., Berg, O. H., Mentes, B., Papaspiropoulos, G., Hansson, H-C., Kulmala, M., Aalto, P., Väkevä, M., Berner, A., Bizjak, M., Fuzzi, S., Laj, P., Facchini, M-C., Orsi, G., Ricci, L., Nielsen, M., Allan, B. J., Coe, H., McFiggans, G., Plane, J. M. C., Collett Jr., J. L., Moore, K. F. and Sherman, D. E. 2000. ACE-2 HILLCLOUD: an overview of the ACE-2 ground based cloud experiment. *Tellus* **52B**, 750–778.

Clegg S. L., Brimblecombe P. and Wexler A. S. 1998. Thermodynamic model of the system H^+–NH_4^+–Na^+–SO_4^{2-}–NO_3^-–Cl^-–H_2O at 298.15 K. *J. Phys. Chem.* **102A**, 2155–2171.

Hoell, C., O'Dowd et al. 2000. Time-scale analysis of marine boundary layer aerosol evolution: Lagrangian case studies under clean and polluted conditions. *Tellus* **52B**, 423–438.

IPCC (Intergovernmental Panel on Climate Change) 1995. *Climate change: the science of climate change* (eds. J. T. Houghton, L. G. Meira Filho, B. A. Callander, N. Harris, A. Kattenberg and K. Maskell). Cambridge University Press, Cambridge.

Johnson, D. W. et al. 2000. An overview of the Lagrangian experiments undertaken during the north Atlantic regional aerosol characterisation experiment (ACE-2). *Tellus* **52B**, 290–320.

Kerminen, V.-M. 1997. The effects of particle chemical character and atmospheric processes on particle hygroscopic properties, *J. Aerosol Sci.* **28**, 121–132.

McMurry, P. H. and Stolzenburg, M. R. 1989. On the sensitivity of particle size to relative humidity for Los Angeles aerosols. *Atm. Env.* **23**, 497–507.

Murphy, D. M., Thomson, D. S., Middlebrook, A. M. and Schein, M. E. 1998. In situ single-particle characterization at Cape Grim, *J. Geophys. Res.* **103**, 16485–16491.

Neusüß, C., Weise, D., Birmili, W., Wex, H., Wiedensohler, A., Covert D. S. 2000. Size-segregated chemical, gravimetric and number distribution derived mass closure of the aerosol in Sagres, Portugal during ACE-2, *Tellus* **52B**, 169–184.

Nilsson, E. D., Rannik, Ü., Swietlicki, E., Aalto, P. P., Zhou, J. and Leck, C. 1998. Turbulent aerosol number fluxes over the sea and pack ice: Deposition and wind driven fluxes of sub micrometer particles, *J. Aerosol Sci.* **29**(S1), 505–506.

O'Dowd, C. D. and Smith, M. H. 1993. Physico-chemical properties of aerosol over the Northeast Atlantic: evidence for wind speed related sub-micron sea-salt aerosol production. *J. Geophys. Res.*, **98**, 1137–1149.

Plinis, C., Pandis, S. N. and Seinfeld, J. H., 1995. Sensitivity of direct climate forcing by atmospheric aerosols to aerosol size and composition. J. Geophys. Res., **100,** 18739–18754.

Putaud, J. P., Van Dingenen, R., Mangoni, M., Virkkula, A., Raes, F., Maring, H., Prospero, J. M., Swietlicki, E. Berg, O. H., Hillamo, R. and Mäkelä T., 2000. Chemical mass closure and origin assessment of the submicron aerosol in the marine boundary layer and the free troposphere at Tenerife during ACE-2. *Tellus* **52B**, 141–168.

Quinn, P. K. et al., 2000. A comparison of aerosol chemical and optical properties from the first and second Aerosol Characterization Experiment. *Tellus* **52B**, 239–257.

Raes, F., Van Dingenen, R., Cuevas, E., Van Velthoven, P. F.J. and Prospero, J. M. 1997. Observations of aerosols in the free troposphere and marine boundary layer of the subtropical Northeast Atlantic: Discussion of processes determining their size distribution. *J. Geophys. Res.*, **98**, 1137–1149.

Raes, F., Bates, T. S., McGovern, F. and Van Liedekerke, M. 2000. The Second Aerosol Characterization Experiment (ACE-2): General context and main results. *Tellus* **52B**, 111–125.

Russell, L. M., Lenschow, D. H., Laursen, K. K., Krummel, P. B., Siems, S. T., Bandy, A. R., Thornton, D. C. and Bates, T. S. 1998. Bidirectional mixing in an

ACE-1 marine boundary layer overlain by a second turbulent layer. *J. Geophys. Res.* **103**, 16411–16432.

Sollazzo, M. J., Russell, L. M., Wood, R., Osborne. S., Percival, D. and Johnson D. W. 2000. Entrainment rates during ACE-2 Lagrangian experiments calculated from aircraft measurements. *Tellus* **52B**, 335–347.

Stull, R. B. 1988. *An introduction to boundary layer meteorology*, 670 pp. Kluwer Acad., Norwell, Mass.

Stratmann F., Orsini D. and Kauffeldt Th. 1997. Inversion algorithm for TDMA measurements, *J. Aerosol Sci.* **28**(S1), 701–702.

Stolzenburg, M. R. and McMurry, P. H. 1988. *TDMAFIT User's Manual.* PTL Publications No.653, Particle Technology Laboratory, Department of Mechanical Eng., University of Minnesota, Minneapolis, MN, USA.

Svenningsson, B., Hansson, H-C., Martinsson, B., Wiedensohler, A., Swietlicki, E., Cederfelt, S-I., Wendisch, M., Bower, K. N., Choularton, T. W. and Colvile, R. N. 1997. Cloud droplet nucleation scavenging in relation to the size and hygroscopic behaviour of aerosol particles. *Atm. Env.* **31**, 2463–2475.

Swietlicki, E., Svenningsson, B., Martinsson, B. G., Berg, O., Frank, G., Cederfeldt, S.-I., Mentes, B., Hansson, H.-C. and Wiedensohler, A. 1997. Hygroscopic properties of continentally influenced atmospheric aerosol particles and their importance for nucleation scavenging. In: *Proceedings of EUROTRAC Symposium '96* (eds: Borrell, P. M., Borrell, P., Kelly, K., Cvitas, T. and Seiler, W.). Computational Mechanics Publications, Southampton, Vol. **1**, 225–229.

Swietlicki, E. Zhou, J., Berg, O. H., Nilsson, E. D., Aalto, P. P. and Leck, C. 1998. Hygroscopic behaviour of aerosol particles in the Arctic marine boundary layer — relation to air mass history and mixing. *J. Aerosol Sci.* **29**(S1), 9–10.

Swietlicki, E., Zhou, J., Berg, O. H., Martinsson, B. G., Frank, G., Cederfelt, S.-I., Dusek, U., Berner, A., Birmili, W., Wiedensohler, A., Yuskiewicz, B. and Bower, K. N. 1999. A closure study of sub-micrometer Aerosol particle hygroscopic behaviour. *Atm. Res.,* **50**, 205–240.

Tang, I. N. 1997. Thermodynamic and optical properties of mixed-salt aerosols of atmospheric importance. *J. Geophys. Res.*, **102**, 1883–1893.

Tang, I. N. and Munkelwitz, H. R. 1994. Water activities, densitites, and refractive indices of aqueous sulfates and sodium nitrate droplets of atmopsheric importance. *J. Geophys. Res.*, **99**, 18801–18808.

Verver, G., Raes, F., Vogelenzang, D. and Johnson, D. 2000. The Second Aerosol Characterization Experiment (ACE-2): Meteorological and chemical context. *Tellus* **52B**, 126–140.

Weingartner, E., Burtscher, H. and Baltensperger, U. 1997. Hygroscopic properties of carbon and diesel soot particles, *Atm. Env.* **31**, 3211–3227.

Zhang, X. Q., McMurry, P. H., Hering, S. V. and Casuccio, G. S., 1993. Mixing characteristics and water content of submicron aerosols measured in Los Angeles and at the Grand Canyon. *Atm. Env.* **27A**, 1593–1607.